

Ultra-bright keV X-ray source generated by relativistic femtosecond laser pulse interaction with thin foils and its possible application for HEDS investigations

A.Y. FAENOV,^{1,2} T.A. PIKUZ,^{2,3} G.A. VERGUNOVA,⁴ S.A. PIKUZ,^{2,5} I.Y. SKOBELEV,^{2,5}
A. ANDREEV,^{6,7} A. ZHIDKOV,³ AND R. KODAMA^{1,3}

¹Open and Transdisciplinary Research Initiatives, Osaka University, Suita, Osaka, Japan

²Joint Institute for High Temperatures, Russian Academy of Sciences, Moscow, Russia

³PPC and Graduate School of Engineering, Osaka University, Yamadaoka, Suita, Osaka, Japan

⁴P.N. Lebedev Physical Institute of the Russian Academy of Sciences, Moscow, Russia

⁵National Research Nuclear University MEPhI, Moscow 115409, Russia

⁶Max Born Institute, Berlin 12489, Max-Born str. 2a, Berlin, Germany

⁷ELI-ALPS, Szeged, Hungary

(RECEIVED 4 May 2017; ACCEPTED 25 May 2017)

Abstract

It was shown (Faenov *et al.*, 2015b) that the energy of femtosecond laser pulses with relativistic intensity approaching to $\sim 10^{21}$ W/cm² is efficiently converted to X-ray radiation and produces exotic states in solid density plasma periphery. We propose and show by one-dimensional two-temperature hydrodynamic modeling, that applying two such unique ultra-bright X-ray sources with intensities above 10^{17} W/cm² – allow to generate shock waves with strength of up to some hundreds Mbar, which could give new opportunities for studies of matter in extreme conditions.

Keywords: High-power lasers; Laser–plasma interactions; X-ray sources; X-ray spectroscopy; High-energy density sciences

1. INTRODUCTION

During past decades, pulsed optical lasers with different intensities were successfully used for creation and study of matter in extreme conditions (Drake, 2006; Fortov, 2016). In this case, the input laser energy is generally transferred to the outer (valence) electrons of the target atoms, as well as to free electrons, which cause heating and generation of shock waves in matter. In contrast, with irradiation by X rays, electrons in the inner shells are ionized first. Such electrons usually have higher energy compared with previous cases, which cause faster heating of the matter and at higher electron temperatures. Additionally, X-ray pulses are more completely and homogeneously absorbed by matter, while absorption of visible laser pulses is typically in the scale of 10th %. This allows transforming X-ray laser energy more effectively into matter, to produce higher strength shock waves, and to have significant lowering of

nanomodification and ablation thresholds compared with heating by optical laser beams including the femtosecond ones.

First experiments, in which X-ray bright sources have been generated in laser-produced plasma, then used for study of X-ray interaction with matter and for radiation-driven ablation as well as for shock wave generation, were already begun about 30 years ago (Endo *et al.*, 1988; Kaiser *et al.*, 1991; Kodama, 1992; von der Linde *et al.*, 2001). Later, X-ray radiation of exploding wires plasma (Fortov *et al.*, 1996) was started to be used for such purposes. Recently, the National Ignition Facility (NIF) team (Fournier *et al.*, 2016), according to the X-ray Transport and Radiation Response Assessment (XTRRA) program, has developed an experimental platform to evaluate the X-ray-generated stress and impulse to provide improved modeling and simulation methods to study impulse and thermostructural response of materials in well-characterized X-ray environments.

Recently, soft X-ray lasers and X-ray free electron lasers (XFEL) X-ray beams reached relatively high intensities and started to be routinely used for investigations of interaction with matter (Faenov *et al.*, 2009; Ishino *et al.*, 2011, 2013;

Address correspondence and reprint requests to: A.Y. Faenov, Open and Transdisciplinary Research Initiatives, Osaka University, Suita, Osaka, Japan. E-mail: anatolyf@hotmail.com

Inogamov *et al.*, 2011; Vinko *et al.*, 2012; Koyama *et al.*, 2013; Yoneda *et al.*, 2014; Starikov *et al.*, 2014). Lately, it was also demonstrated (Colgan *et al.*, 2013, 2016; Pikuz *et al.*, 2013, 2017; Hansen *et al.*, 2014; Faenov *et al.*, 2015a, b) that conventional optical lasers with pulse duration of 30–1000 fs and laser intensity $(0.3\text{--}1.0) \times 10^{21}$ W/cm² irradiating thin aluminum (Al) or Si (silicon) foils could generate very bright X-ray radiation with intensities exceeding 10^{17} W/cm² (see Fig. 1). Interaction of such highly intensive X-ray radiation with cold periphery of laser spot efficiently produces exotic states of matter – hollow ions (Skobelev *et al.*, 2012) and could generate shock waves with a very high pressure.

Here we briefly discuss some previous results obtained by (Faenov *et al.*, 2015), which demonstrated that interaction of femtosecond laser pulses with intensity $\sim 10^{21}$ W/cm² with thin Al foils allowed to produce X-ray radiation with intensity exceeding 10^{17} W/cm². We also propose to use two such laser systems, which will generate two separated bright point X-ray sources. In such case, it will be possible to generate between such X-ray sources the shock waves with strengths of some hundreds Mbar. Providing one-dimensional (1D) modeling results support such proposal.

2. GENERATION OF ULTRA-BRIGHT X-RAY SOURCE BY FEMTOSECOND ULTRA-INTENSE LASER PULSES INTERACTION WITH THIN FOILS

First demonstration (Colgan *et al.*, 2013; Pikuz *et al.*, 2013; Hansen *et al.*, 2014) that the energy of laser pulses with relativistic intensity higher than 10^{20} W/cm² could be efficiently converted into X-ray radiation with intensities higher than 10^{18} W/cm² was done for the case of using Vulcan PW laser facility of Rutherford laboratory for laser

pulse duration ~ 1 ps and large laser energy on the target. Unfortunately such laser systems have serious drawback – low repetition rate. For practical applications, Ti:Sa femtosecond laser systems (Kiryama *et al.*, 2015; Astra-Gemini WEB page ‘<https://www.clf.stfc.ac.uk/Pages/The-Astra-Gemini-Facility.aspx>’) are more attractive, because they allowed to reach even higher laser intensity on the target and provide repetition rate up to 1 Hz nowadays. That is why we propose to use such laser systems for generation of bright X-ray sources and use them in high-energy dense science investigations.

The experiments discussed (Faenov *et al.*, 2015) were performed using the J-KAREN (Kiryama *et al.*, 2010), an optical parametric chirped-pulse amplification Ti:Sapphire hybrid laser system delivered energy on the target up to ~ 7 J with laser pulse duration of 35 fs and a typical contrast of 10^{10} . Using F/2.1 off-axis parabolic mirror, *p*-polarized laser pulses with energies from 0.4 to 7 J were focused onto an Al foils with thickness 0.8, 2, 3, 6 μm at an incidence angle of 84° , producing a spot with the full width half maximum (FWHM) diameter of ~ 4.5 μm and the peak laser intensity of 10^{21} W/cm². Diagnostic of produced plasma parameters was performed by high-resolution spectroscopy measurements (see Fig. 2a) using a focusing spectrometer with spatial resolution. The instrument was equipped by spherically bent mica crystal with a lattice spacing $2d \sim 19.94$ Å and a radius of curvature of $R = 150$ mm. The crystal was aligned to operate at $m = 2$ of reflection to record *K*-shell emission spectra of multi-charged (He_α line of Al XII and Ly_α line of Al XIII) and neutral (i.e., K_α line) Al ions in 6.8–8.43 Å wavelength range, that is, energy range from 1.45 to 1.85 keV. Simultaneously in third order of mica crystal reflection, recombination continuum in 2210–2730 eV energy range was registered (see raw data, which includes typical spectra from both mica crystal orders in Fig. 2b).

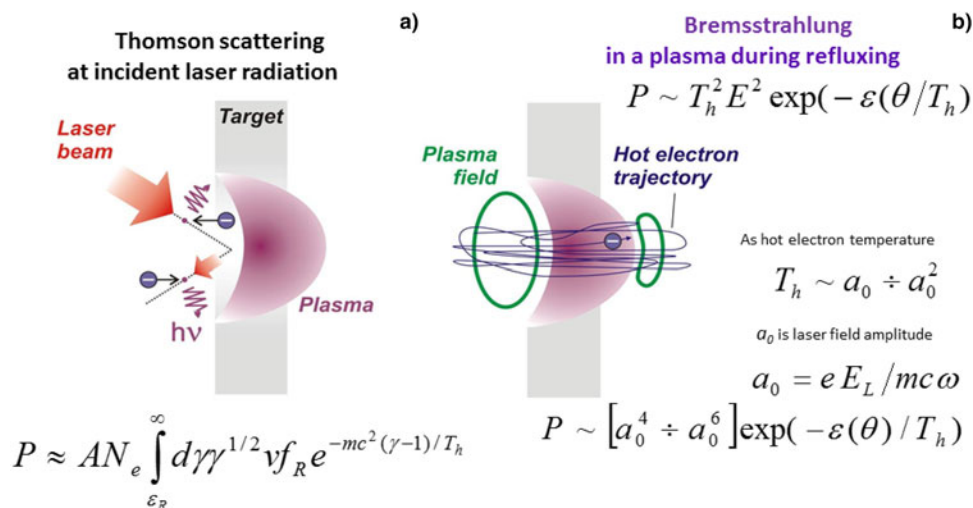


Fig. 1. Generation of ultra-intense X-ray source with intensities $P \sim 10^{17\text{--}18}$ W/cm² in plasma irradiated by relativistic laser pulses with intensities above 10^{20} W/cm². (a) X-ray generation by Thomson scattering at incident laser radiation; (b) X-ray generation by bremsstrahlung in a plasma during electron refluxing.

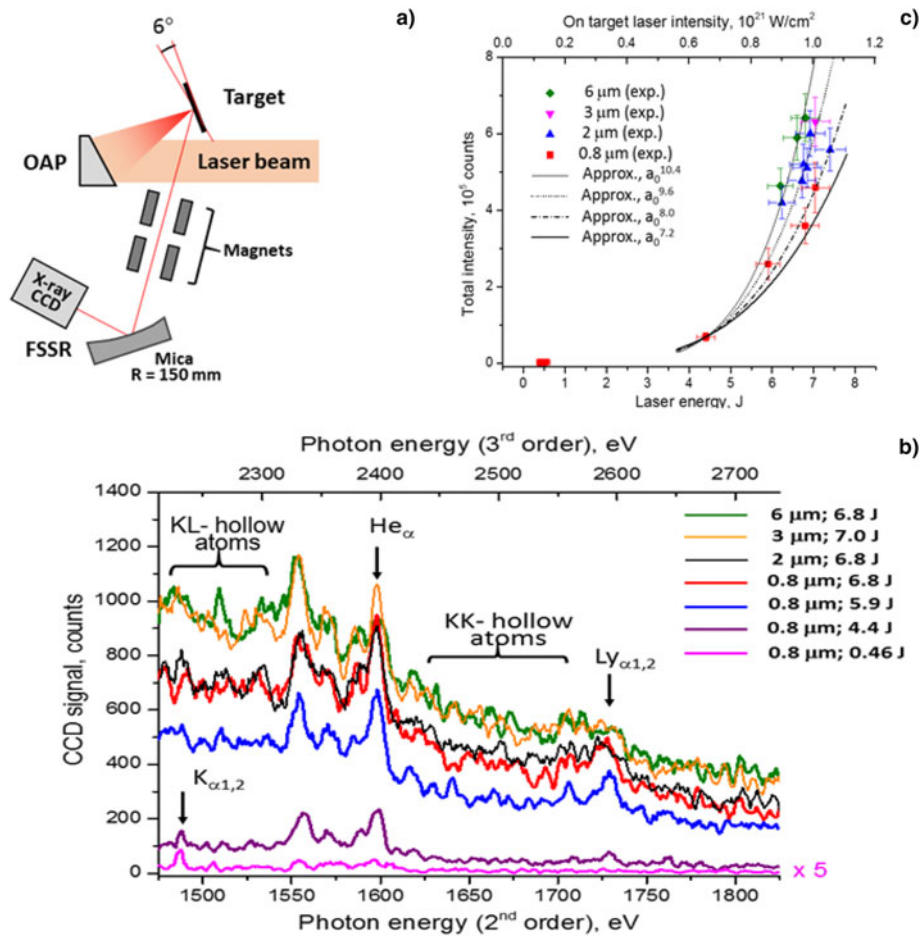


Fig. 2. Scheme of observation and results. (a) Experimental set up. Laser beam focused by off-axis parabola practically perpendicular to the surface of foil and heat plasma. Produced plasma generated X-ray emission, which was measured by X-ray high luminosity spectrometer with high spectral resolution placed at 45° to the target surface. (b) Single shot, spatially and temporally averaged Al ions K-shell spectra (raw data) (Faenov *et al.*, 2015) emitted from foil targets with different thickness and laser energies (intensity of spectra obtained by irradiation of laser pulse with energy 0.46 J is multiplied by factor 5). (c) Intensity of X-ray emission observed at X-ray CCD integrated over the energy range 1450–1850 and 2210–2730 eV versus the laser intensity for Al foils with different thickness (Faenov *et al.*, 2015).

The green, yellow, black, and red curves represent the data obtained from 6, 3, 2 and 0.8 μm Al foils, respectively, irradiated by laser pulses with 6.8–7.0 J on the target. In such case, the laser intensity at the central area of the focal spot of 4.5 μm diameter reached $\sim 1.0 \times 10^{21}$ W/cm². For comparison, spectra observed for lower pulse energies, down to 0.46 J, from Al target with thickness of 0.8 μm are also presented. It is necessary to mention that very high intensity of plasma radiation spectra, shown in Figure 2b, were measured in a single laser shot despite the fact that X-ray spectrometer detector was placed at the distance >2000 mm from the plasma. The total X-ray intensity was measured by an X-ray charge coupling device (CCD) as a sum of intensities in the energy ranges ~ 1450 – 1850 and 2210 – 2730 eV. Usually, the X-ray intensity in these ranges grows very slowly and almost linearly with the laser pulse intensities. However, a strong, non-linear behavior of the X-ray radiation power on the energy of incident laser beams is clearly seen in Figure 2c

in our experiments for the intensities over $I \sim 6 \times 10^{20}$ W/cm². As it was demonstrated in Faenov *et al.* (2015a), this indicates that collisionless strong X-ray radiation, initiated by energetic electrons in the laser focal spot, becomes dominant. Increasing the laser intensity causes not only an increase in the X-ray spectral intensity, but also the appearance of new line features indicative of high X-ray flux interacting with high-density plasma. The emergence of intense emission lines, due to transitions from levels when both K-shell electrons are absent (so called KK “hollow ions”) (see Figs 2b and 3a) which are located between He_α and Ly_α clearly indicates that, at these laser intensities, there are significant X-ray pumping of the peripheral plasma from the central plasma resulting in photoionization of Al ions. Modeling of KK hollow-ion spectra of Al (see for details Colgan *et al.*, 2013; Hansen *et al.*, 2014; Faenov *et al.*, 2015a) shows that radiation temperature T_r of such bright X-ray source should be in the level of ~ 1.5 – 3 keV. As it could be seen from Figure 3b the fact of observation of KK hollow ions of different ions allowed one to

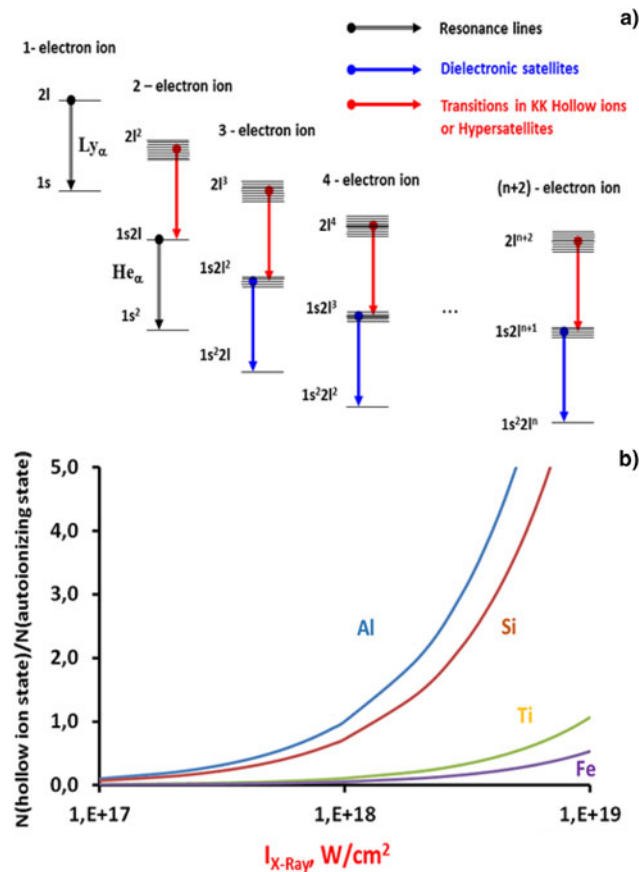


Fig. 3. (a) Scheme of energy levels of multi-charged ions; (b) efficiency of KK hollow ions photoionization by external X-ray source for different ionic charges. The fact of observation of KK hollow ions of different ions allowed one to estimate the value of X-ray source intensity.

estimate the value of X-ray source intensity. For the case of Al plasma, KK hollow ions could be observed with X-ray pumping intensity exceeded 10^{17} W/cm².

Our investigations show that observable features of the hollow-ion spectra are sensitive to such plasma parameters as density, temperature, hot-electron fraction, and intensity of the X-ray pumping radiation and could be used for effective diagnostics of warm dense matter parameters.

At the same time, absorption of such ultra-bright X-ray intensity at the periphery of laser spot should cause very strong shock waves, which could be used for investigations of matter modification dynamics and other aspects of high-energy density science studies. If to focus two laser beams in the nearby spots, the strength of the produced shock waves will be even higher. It is necessary to mention that the laser Astra-Gemini facility (RAL, UK) has already two beams with parameters allowing reaching laser intensity $\sim 10^{21}$ W/cm² on the target. Recently at the XFEL SACLA (Spring-8, Japan) facility, two sub-PW laser systems are being commissioned, making it interesting to consider what strengths of shock waves could be reached if such two laser beams will be focused relatively close to one another at the surface of thin foils.

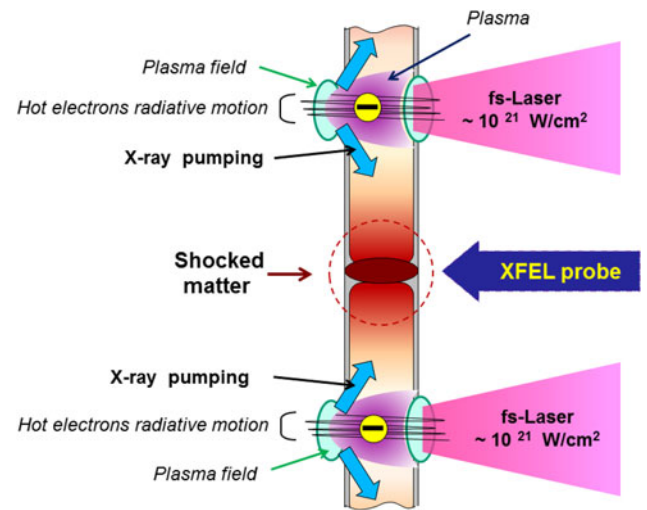


Fig. 4. Generation of two ultra-intense X-ray sources in plasma irradiated by relativistic laser pulses with intensities $\sim 10^{21}$ W/cm². Bright X-ray sources with intensities exceeding 10^{17} W/cm² will irradiate foil between two sources and produce strong shock waves. XFEL or any other X-ray probe beam could be used to probe the created exotic matter.

A possible scheme of such an experiment is presented in Figure 4. XFEL Probe beam could be used both from front and rear side of target irradiated by two pump laser beams. We performed 1D two-temperature hydrodynamic modeling to estimate potential strength of shock waves, which could be generated between two irradiated laser spots.

3. SIMULATION OF OVERHEATED SOLID-STATE MATTER UNDER THE X-RAY RADIATION BY TWO-TEMPERATURE HYDRODYNAMIC CODE

Formation of an overheated solid-state matter under the X-ray radiation is simulated by 1D numerical code RADIANT (Govorun *et al.*, 1986). A physical-mathematical model for the RADIANT is comprised of the two-temperature hydrodynamic equations, namely, motion equation, continuity equation, energy variation equation for the electron and ion components, and equations of state for ions and electrons. The electron-ion exchange, classical or reduced Spitzer heat conductivity have been taken into account. Equation for a two-temperature gas dynamics is solved jointly with a multi-group energy transfer equation for 96 groups. Fragmentation of the radiation energy spectrum into spectral groups is varied. The simulation results prove to be stable to such variations. In these simulations, we used optical coefficients of absorption calculated by the THERMOS code (Nikiforov *et al.*, 2000). Temperature of the laser-heated Al layers is estimated to be of 1.5 keV. Respectively, the maximum of the Planck function falls on the quantum energy of 4.5 keV. Due to the optical thickness of the plasma, Planck spectrum is modified as it is shown in Figure 5 and then heated the periphery of plasma. The range of the spectral energies up to 15 keV has been taken into account in the numerical

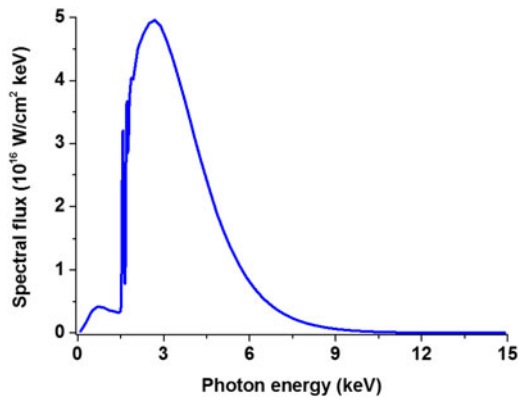


Fig. 5. The radiation spectral flux incident onto the cold Al layer from the hot boundary.

calculations, which exceeds the range of quantum energies observed experimentally.

The quanta originated from the laser-heated regions (Fig. 6, regions I and III) are absorbed in a neighbor cold region II of Al. As the heating advances, these layers become the sources of the soft X-ray radiation. Thus, the energy is transferred from one plasma layer to another by means of the radiation. The mean free path for different quanta is different. The quanta of different energy are heating up the plasma to a different value.

It is necessary to mention that in the discussed scheme of irradiation, the geometry of heating the plasma layer located between the hot spots is not 1D. Along the central curve, which connects the hot spots and is parallel to the free boundaries of the heated area, the lateral expansion is absent. In the noted area, the plasma is heated by the counter propagating radiative fluxes. Maximal velocity of the heated Al plasma-free boundary expansion can be estimated from the relation of gas expansion into the vacuum (Zel'dovich & Raizer, 1966)

$$u = \frac{2}{\gamma - 1} c_s,$$

where sound velocity is $c_s = \sqrt{\gamma(P/\rho)}$ and γ is the adiabaticity coefficient. The estimates show that the expansion velocity of

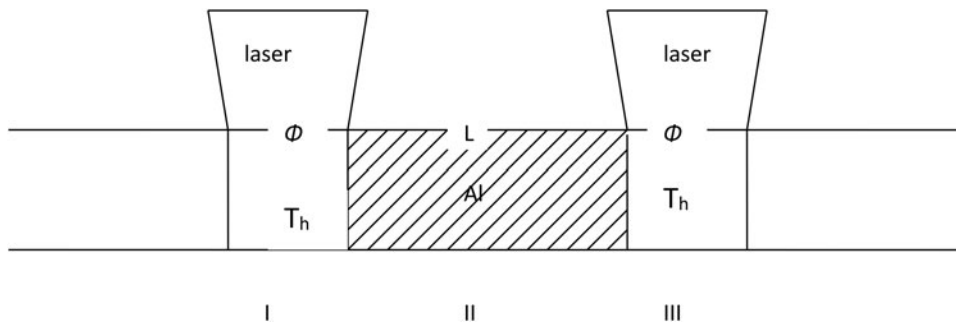


Fig. 6. The scheme of numerical simulation geometry. At the initial time moment, the areas I and III are heated up to T_h , 1.5 keV. The Al initial density is 2.7 g/cm³. The distance between the heated layers L is varied.

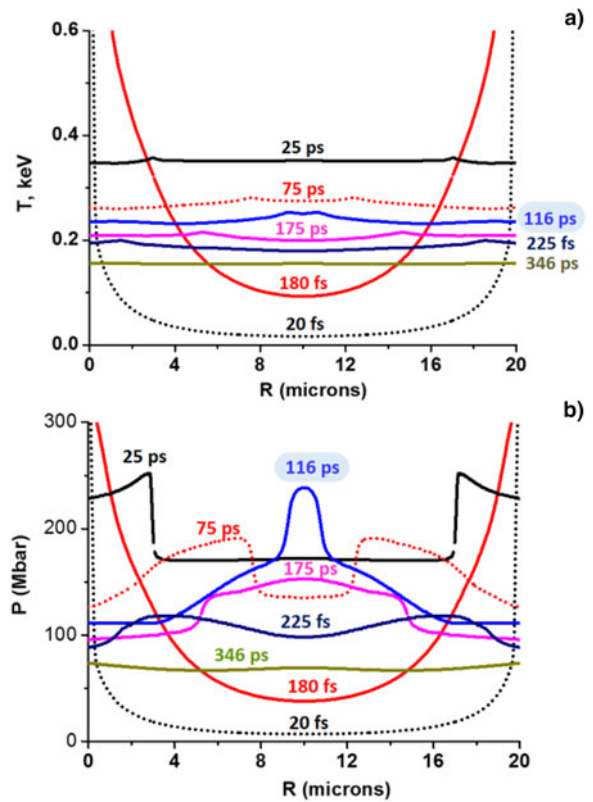


Fig. 7. The temperature (a) and pressure (b) profiles formed in the plasma plane layer up to the time moments 20, 180 fs, 25, 75, 116, 175, 225, and 346 ps.

the laser-heated plasma spots is $\sim 10^7$ cm/s. The expansion velocity of the Al layer heated by the radiation coming from the hot spots is half as much. This means that the free boundary of this layer will expand by 5 μ m during 100 ps. One may consider that 1D approximation is applicable to such time values, and can assume that 1D analysis gives notion about the formation of pressure jumps in the plasma.

A series of 1D calculations have been made for the Al of 2.7 g/cm³ density in the plane geometry, as shown in Figure 6. The distance L between the hot spots of the heated-up Al was varied.

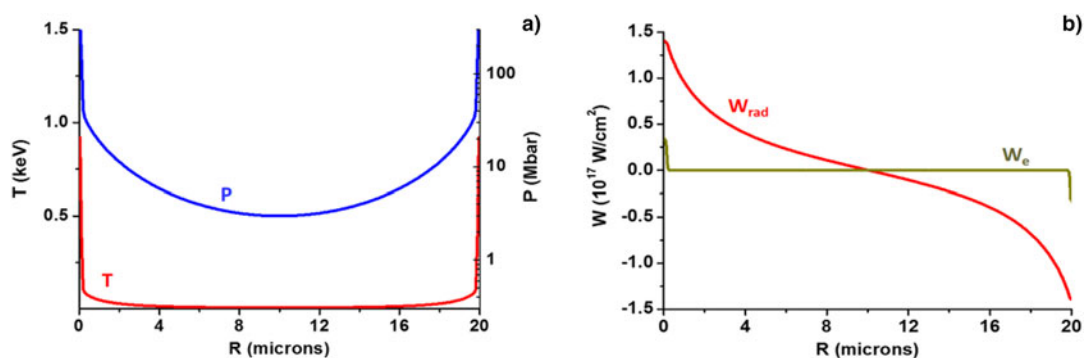


Fig. 8. The temperature T and pressure P profiles (a), and the radiative W_{rad} and electron heat-conductivity W_e fluxes (b) at the time moment 10 fs in the plane Al layer $L = 20 \mu\text{m}$ (the area II in Fig. 6). Positive fluxes are heating the cold Al from the left boundary, and the negative fluxes are heating cold Al from the right boundary.

The heating evolution of an Al layer is illustrated in the example of a layer of $L = 20 \mu\text{m}$ distance. The spectral flux coming from the hot boundary to the cold Al layer has the maximum at the quanta energy of 2.5 keV and drops rather sharply on both sides of the spectrum (Fig. 7). The spectral integral flux is $\sim 10^{17} \text{ W/cm}^2$. Up to 280 fs, the flux intensity drops by ~ 10 times.

By the time of 180 fs, under the action of such a high-power flux, the temperature of the initially cold layer exceeds 100 eV (Fig. 7). The pressure is growing as well. Then the pressure jumps formed by the radiation propagate into the heated matter (25, 75 ps). At $t = 116$ ps, the pressure jumps collapse in the center, the pressure reaches 240 Mbar, and then the unloading waves come from the center.

Figure 8 illustrates the temperature and pressure profiles, as well as the radiative flow and the electron heat-conductivity flow in a heated Al layer at the moment 10 fs. Negative values of the flux correspond to the heating of cold Al from the right-hand boundary. The depth of electron heat-conductivity flux penetration into the cold Al is minor compared with the flux of self-radiation from the Al hot spots (Fig. 8b). The penetration of the heating radiation into the cold matter depends on the spectral energy of the radiation. As a result of plasma radiative exposure, the plasma self-radiation flow from the hot spots is decreased dramatically and ~ 10 times smaller by the time of 280 fs.

The Table 1 presents some of the results from numerical modeling of the plane Al layer heating depending on the distance L between the hot spots. Here P_{max} is the maximum

Table 1. Results of modeling for different distances between two separated X-ray sources.

L (μm)	10	20	40
P_{max} (Mbar)	300	240	180
$t(P_{\text{max}})$ (ps)	50	110	250
T_e (eV)	300	250	210

pressure in the center of a cold Al layer at the time moment $t(P_{\text{max}})$; T_e , the electron temperature of the layer at this time.

4. CONCLUSION

Recent experiments demonstrated that the energy of subpicosecond or femtosecond laser pulses with relativistic intensity approaching to $\sim 10^{21} \text{ W/cm}^2$ is efficiently converted to keV X-ray radiation with intensities exceeding 10^{17} W/cm^2 . Our 1D two-temperature hydrodynamic simulations have shown that within the frames of the discussed geometry, the formation of high-pressure plasma is possible under the action of X-ray radiation produced by relativistic intensity laser interaction with thin foils. The life time of such plasma is $\lesssim 100$ ps, since the lateral expansion and radiative energy losses destruct the plasma. It will be very interesting to provide experimental investigations of various material deformation dynamic and other aspects of high-energy density science under such a strong shock wave generation by using XFEL or any other hard X-ray probe instruments in the future experiments. Combining these ultra-bright laser plasma-produced X-ray sources and XFEL probe observations can provide much greater detail than had previously been possible, probing ultra-fast lattice-level dynamical phenomena and transient states associated with hundreds Mbar shock compression, including laser ablation, shock formation, and phase transformations, which are all difficult to predict with only simulations.

ACKNOWLEDGMENT

The work is partly done in the frame of State Assignment for JIHT RAS (project No. 0044-2014-0003).

REFERENCES

- COLGAN, J., ABDALLAH JR., J., FAENOV, A.Y., PIKUZ, S.A., WAGENAARS, E., BOOTH, N., CULFA, O., DANCE, R.J., EVANS, R.G., GRAY, R.J., KAEMPFER, T., LANCASTER, K.L., MCKENNA, P.,

- ROSSALL, A.L., SKOBELEV, I.Y., SCHULZE, K.S., USCHMANN, I., ZHIDKOV, A.G. & WOOLSEY, N.C. (2013). Exotic dense matter states pumped by relativistic laser plasma in the radiation dominant regime. *Phys. Rev. Lett* **110**, 125001.
- COLGAN, J., FAENOV, A.Y., PIKUZ, S.A., TUBMAN, E., BUTLER, N.M.H., ABDALLAH JR., J., DANCE, R.J., PIKUZ, T.A., SKOBELEV, I.Y., ALKHIMOVA, M.A., BOOTH, N., GREEN, J., GREGORY, C., ANDREEV, A., LÖTZ, R., USCHMANN, I., ZHIDKOV, A., KODAMA, R., MCKENNA, P. & WOOLSEY, N. (2016). Evidence of high-n hollow-ion emission from Si ions pumped by ultraintense X-rays from relativistic laser plasma. *EPL* **114**, 35001.
- DRAKE, R.P. (2006). *High-Energy-Density Physics: Fundamentals*. Berlin, Heidelberg, New York: Springer.
- ENDO, T., SHIRAGA, H., SHIHOYAMA, K. & KATO, Y. (1988). Generation of a shock wave by soft-X-ray-driven ablation. *Phys. Rev. Lett.* **60**, 1022–1025.
- FAENOV, A.Y., COLGAN, J., HANSEN, S.B., ZHIDKOV, A., PIKUZ, T.A., NISHIUCHI, M., PIKUZ JR., S.A., SKOBELEV, I.Y., ABDALLAH JR., J., SAKAKI, H., SAGISAKA, A., PIROZHKOVA, A.S., OGURA, K., FUKUDA, Y., KANASAKI, M., HASEGAWA, N., NISHIKINO, M., KANDO, M., WATANABE, Y., KAWACHI, T., MASUDA, S., HOSOKAI, T., KODAMA, R. & KONDO, K. (2015a). Nonlinear increase of X-ray intensities from thin foils irradiated with a 200 TW femtosecond laser. *Sci. Rep.* **5**, 13436.
- FAENOV, A.Y., INOGAMOV, N.A., ZHAKHOVSKII, V.V., KHOKHLOV, V.A., NISHIHARA, K., KATO, Y., TANAKA, M., PIKUZ, T.A., KISHIMOTO, M., ISHINO, M., NISHIKINO, M., NAKAMURA, T., FUKUDA, Y., BULANOV, S.V. & KAWACHI, T. (2009). Low-threshold ablation of dielectric irradiated by picosecond soft X-ray laser pulses. *Appl. Phys. Lett.* **94**, 231107.
- FAENOV, A.Y., SKOBELEV, I.Y., PIKUZ, T.A., PIKUZ JR., S.A., KODAMA, R. & FORTOV, V.E. (2015b). Diagnostics of warm dense matter by high-resolution X-ray spectroscopy of hollow ions. *Laser Part. Beams* **33**, 27–39.
- FORTOV, V.E. (2016). *Extreme States of Matter. High Energy Density Physics*. 2nd edn. Switzerland: Springer International Publishing.
- FORTOV, V.E., DYABILIN, K.S., LEBEDEV, M.E., SMIRNOV, V.P. & GRABOVSKII, E.V. (1996). Shock wave excitation by soft X-rays. *Laser Part. Beams* **14**, 789–792.
- FOURNIER, K.B., BROWN JR., C.G., YEOMAN, M.F., FISHER, J.H., SEILER, S.W., HINSHELWOOD, D., COMPTON, S., HOLDENER, F.R., KEMP, G.E., NEWLANDER, C.D., GILLIAM, R.P., FROULA, N., LILLY, M., DAVIS, J.F., LERCH, M.A., & BLUE, B.E. (2016). X-ray transport and radiation response assessment (XTRRA) experiments at the National Ignition Facility. *Rev. Sci. Instrum.* **87**, 11D421.
- GOVORUN, T.K., EVSEEV, G.A. & MISHCHENKO, T.V. (1986). *The RADIANT Program for the Modeling of One-Dimensional Spherically Symmetric Tasks of the Radiation Gas Dynamics Preprint No. 176, IPM im. M. V. Keldysha AN SSSR*. Moscow: Keldysh Institute of Applied Mathematics of the Academy of Sciences of the Soviet Union.
- HANSEN, S.B., COLGAN, J., FAENOV, A.Y., ABDALLAH JR., J., PIKUZ JR., S.A., SKOBELEV, I.Y., WAGENAARS, E., BOOTH, N., CULFA, O., DANCE, R.J., TALLENTS, G.J., EVANS, R.G., GRAY, R.J., KAEMPFER, T., LANCASTER, K.L., MCKENNA, P., ROSSALL, A.K., SCHULZE, K.S., USCHMANN, I., ZHIDKOV, A.G. & WOOLSEY, N.C. (2014). Detailed analysis of hollow ions spectra from dense matter pumped by X-ray emission of relativistic laser plasma. *Phys. Plasmas* **21**, 031213.
- INOAMOV, N.A., FAENOV, A.Y., ZHAKHOVSKY, V.V., PIKUZ, T.A., SKOBELEV, I.Y., PETROV, Y.V., KHOKHLOV, V.A., SHEPELEV, V.V., ANISIMOV, S.I., FORTOV, V.E., FUKUDA, Y., KANDO, M., KAWACHI, T., NAGASONO, M., OHASHI, H., YABASHI, M., TONO, K., SENDA, Y., TOGASHI, T. & ISHIKAWA, T. (2011). Two-temperature warm dense matter produced by ultrashort extreme vacuum ultraviolet-free electron laser (EUV-FEL) pulse. *Contrib. Plasma Phys.* **51**, 419–426.
- ISHINO, M., FAENOV, A.Y., TANAKA, M., HASEGAWA, N., NISHIKINO, M., TAMOTSU, S., PIKUZ, T.A., INOGAMOV, N.A., ZHAKHOVSKY, V.V., SKOBELEV, I.Y., FORTOV, V.E., KHOKHLOV, V.A., SHEPELEV, V.V., OHBA, T., KAIHORI, T., OCHI, Y., IMAZONO, T. & KAWACHI, T. (2011). Nanoscale surface modifications and formation of conical structures at aluminum surface induced by single shot exposure of soft X-ray laser pulse. *J. Appl. Phys.* **109**, 013504.
- ISHINO, M., FAENOV, A.Y., TANAKA, M., TAMOTSU, S., HASEGAWA, N., NISHIKINO, M., PIKUZ, T.A., KAIHORI, T. & KAWACHI, T. (2013). Observations of surface modifications induced by the multiple pulse irradiation using a soft picosecond X-ray laser beam. *Appl. Phys. A* **110**, 179–188.
- KAISER, N.M., MEYER-TER-VEHN, J. & RAMIS, R. (1991). Numerical study of an X-ray driven carbon foil. *Laser Part. Beams* **9**, 759–768.
- KIRIYAMA, H., MORI, M., NAKAI, Y., SHIMOMURA, T., SASAO, H., TANOUÉ, M., KANAZAWA, S., WAKAI, D., SASAO, F., OKADA, H., DAITO, I., SUZUKI, M., KONDO, S., KONDO, K., SUGIYAMA, A., BOLTON, P.R., YOKOYAMA, A., DAIDO, H., KAWANISHI, S., KIMURA, T. & TAJIMA, T. (2010). High temporal and spatial quality petawatt-class Ti:Sapphire chirped-pulse amplification laser system. *Opt. Lett.* **35**, 1497–1499.
- KIRIYAMA, H., MORI, M., PIROZHKOVA, A.S., OGURA, K., SAGISAKA, A., KON, A., ERISKEPOV, T.Z., HAYASHI, Y., KOTAKI, H., KANASAKI, M., SAKAKI, H., FUKUDA, Y., KOGA, J., NISHIUCHI, M., KANDO, M., BULANOV, S.V., KONDO, K., BOLTON, P.R., SLEZAK, O., VOJNA, D., SAWICKA-CHYLA, M., JAMBUNATHAN, V. & MOCEK, T. (2015). High-contrast, high-intensity Petawatt-class laser and applications. *IEEE J. Sel. Top. Quantum Electron.* **21**, 232–249.
- KODAMA, R. (1992). Study of X-ray laser interaction plasmas. *Laser Part. Beams* **10**, 821–826.
- KOYAMA, T., YUMOTO, H., SENBA, Y., TONO, K., SATO, T., TOGASHI, T., INUBUSHI, Y., KATAYAMA, T., KIM, J., MATSUYAMA, S., MIMURA, H., YABASHI, M., YAMAUCHI, K., OHASHI, H. & ISHIKAWA, T. (2013). Investigation of ablation thresholds of optical materials using 1- μm -focusing beam at hard X-ray free electron laser. *Opt. Express* **21**, 15382.
- NIKIFOROV, A.F., NOVIKOV, V.G. & UVAROV, V.B. (2000). *Quantum-Statistical Models of High-Temperature Plasma*. Moscow: Fizmatlit [in Russian].
- PIKUZ, S.A., SKOBELEV, I.Y., ALKHIMOVA, M.A., POKROVSKII, G.V., COLGAN, J., PIKUZ, T.A., FAENOV, A.Y., SOLOVIEV, A.A., BURDONOV, K.F., EREMEEV, A.A., SLADKO, A.D., OSMANOV, R.R., STARODUBTSEV, M.V., GINZBURG, V.N., KUZ'MIN, A.A., SERGEEV, A.M., FUCHS, J., KHAZANOV, E.A., SHAIKIN, A.A., SHAIKIN, I.A. & YAKOVLEV, I.V. (2017). Formation of a plasma with the determining role of radiative processes in thin foils irradiated by a pulse of the PEARL subpetawatt laser. *JETP Letters* **105**, 13–17.
- PIKUZ JR., S.A., FAENOV, A.Y., COLGAN, J., DANCE, R.J., ABDALLAH, J., WAGENAARS, E., BOOTH, N., CULFA, O., EVANS, R.G., GRAY, R.J., KAEMPFER, T., LANCASTER, K.L., MCKENNA, P., ROSSALL,

- A.L., SKOBELEV, I.Y., SCHULZE, K.S., USCHMANN, I., ZHIDKOV, A.G. & WOOLSEY, N.C. (2013). Measurement and simulations of hollow atom X-ray spectra of solid-density relativistic plasma created by high-contrast PW optical laser pulses. *High Energy Density Phys.* **9**, 560.
- SKOBELEV, I.Y., FAENOV, A.Y., PIKUZ, T.A. & FORTOV, V.E. (2012). Hollow ions spectra in high density laser plasma. *Phys.-Usp.* **182**, 9.
- STARIKOV, S.V., FAENOV, A.Y., PIKUZ, T.A., SKOBELEV, I.Y., FORTOV, V.E., TAMOTSU, S., ISHINO, M., TANAKA, M., HASEGAWA, N., NISHIKINO, M., KAIHORI, T., IMAZONO, T., KANDO, M. & KAWACHI, T. (2014). Soft picosecond X-ray laser nanomodification of gold and aluminum surfaces. *Appl. Phys. B* **116**, 1005–1016.
- VINKO, S.M., CIRICOSTA, O., CHO, B.I., ENGELHORN, K., CHUNG, H.-K., BROWN, C.R.D., BURIAN, T., CHALUPSKÝ, J., FALCONE, R.W., GRAVES, C., HÁJKOVÁ, V., HIGGINBOTHAM, A., JUHA, L., KRZYWINSKI, J., LEE, H.J., MESSERSCHMIDT, M., MURPHY, C.D., PING, Y., SCHERZ, A., SCHLOTTER, W., TOLEIKIS, S., TURNER, J.J., VYSIN, L., WANG, T., WU, B., ZASTRAU, U., ZHU, D., LEE, R.W., HEIMANN, P.A., NAGLER, B. & WARK, J.S. (2012). Creation and diagnosis of a solid-density plasma with an X-ray free-electron laser. *Nature* **482**, 59–62.
- VON DER LINDE, D., SOKOLOWSKI-TINTEN, K., BLOME, CH., DIETRICH, C., ZHOU, P., , C. TARASEVITCH, A., CAVALLERI, A., SIDERS, C.W., BARTY, C.P.J., SQUIER, J., WILSON, K.R., USCHMANN, I. & FÖRSTER, E. (2001). Generation and application of ultrashort X-ray pulses. *Laser Part. Beams* **19**, 15–22.
- YONEDA, H., INUBUSH, I.Y., YABASHI, M., KATAYAMA, T., ISHIKAWA, T., OHASHI, H., YUMOTO, H., YAMAUCHI, K., MIMURA, H. & KITAMURA, H. (2014). Saturable absorption of intense hard X-rays in iron. *Nat. Commun.* **5**, 5080.
- ZEL'DOVICH, Y.B. & RAIZER, Y.P. (1966) *Physics of Shock Waves and High-Temperature Hydrodynamic Phenomena*. New York: Academic Press. Inc.